Biogeochemistry (2009) 95:61–76
DOI 10.1007/s10533-009-9325-9

A comparison of water and carbon dioxide exchange at a windy alpine tundra and subalpine forest site near Niwot Ridge, Colorado

Peter D. Blanken · Mark W. Williams · Sean P. Burns · Russell K. Monson · John Knowles · Kurt Chowanski · Todd Ackerman

Received: 15 September 2008 / Accepted: 7 April 2009 / Published online: 23 April 2009

Abstract Eddy covariance measurements of the surface energy balance and carbon dioxide exchange above high-elevation (3,480 m above sea level) alpine tundra located near Niwot Ridge, Colorado, were compared to simultaneous measurements made over an adjacent subalpine forest over two summers and one winter, from June 9, 2007 to July 3, 2008. The surface energy balance closure at the alpine site averaged 71 and 91%, winter and summer, respectively, due to the high wind speeds, short turbulent flux footprint, and relatively flat ridge-top location of the measurement site. Throughout the year, the alpine site was cooler with higher relative humidity, and had a higher horizontal wind speed, especially in winter, compared to the forest site. Wind direction was persistently downslope at the alpine site (summer and winter, day and night), whereas upslope winds were common at the forest site during summer daytime periods. The latent and sensible heat fluxes were consistently larger in magnitude at the forest site, with the largest differences during summer. The horizontal advective flux of CO_2 at the alpine site averaged 6% of the net ecosystem exchange (*NEE*) during summer nights (5% during summer daytime), and was small in relation to the high wind speeds, relatively flat site, and weak sources of CO_2 upwind of the site. The magnitudes and diurnal behavior of the alpine *NEE* calculated using three methods; eddy-covariance, friction velocity filter, and with advection and storage calculations, gave similar results. The period of net CO_2 uptake (negative *NEE*) was 100 days at the alpine site with a net uptake of 16 g C m^{-2}, compared to 208 days at the forest site with a net uptake of 108 g C m^{-2}, with initiation of net uptake coinciding with air temperatures reaching +10°C. Winter respiration loss at the alpine site was 164 g C m^{-2} over 271 days, compared to 52 g C m^{-2} over 175 days at the forest site, with the initiation of net loss coinciding with air temperatures reaching −10°C at each site.

Keywords Alpine · Carbon · Eddy correlation · Evaporation · Niwot Ridge · Water

P. D. Blanken (✉) · M. W. Williams · J. Knowles
Department of Geography, University of Colorado at Boulder, UCB 260, Boulder, CO 80309-0260, USA
e-mail: blanken@colorado.edu

M. W. Williams · J. Knowles · K. Chowanski · T. Ackerman
Institute of Arctic and Alpine Research, University of Colorado at Boulder, UCB 450, Boulder, CO 80309-450, USA

S. P. Burns
Department of Ecology and Evolutionary Biology, University of Colorado, Boulder, CO, USA

S. P. Burns
National Center for Atmospheric Research, Boulder, CO, USA

R. K. Monson
Department of Ecology and Evolutionary Biology and Cooperative Institute for Research in Environmental Sciences, University of Colorado, Boulder, CO 80309-0334, USA

Introduction

Nearly half of the Earth's terrestrial surface is located 500 m above sea level, with 25% of the Earth's terrestrial surface classified as having mountain relief (Barry 2008). Much of this mountain terrain can be considered "complex terrain", with dramatic changes in elevation, slope, geology, topography, climate, soils, and vegetation over short horizontal distances. Areas of high-elevation complex terrain are known to influence regional climate (e.g. orographic precipitation, rain shadows, mountain waves, valley/mountain breezes, etc.), thus these regions play a major role in the supply of water resources to the surrounding areas. Due to the large influence of these regions on climate and resources, an understanding of the interaction between the surface and vegetation with the lower atmosphere is important. The exchange of energy, water, and carbon between the surface and atmosphere represents the lower boundary conditions which help govern the climate system. Both empirical model estimates and remote-sensing observations in complex terrain suffer from errors associated with poor spatial resolution that cannot capture the surface spatial heterogeneity, and thus lack an understanding of surface processes that are required to properly run and calibrate models.

Additionally, mountain regions have recently been appreciated as sensitive ecosystems, thus observations in these regions over the last 20–50 years may serve as early warning indicators of global environmental changes (Williams et al. 2002; Seastedt et al. 2004). For example, observations of vegetation dynamics at the alpine tree line have indicated changes in species composition (e.g. Elliot and Baker 2004; Keller et al. 2000; Pauli et al. 2001; Walther et al. 2005), increased growth rates (e.g. Paulsen et al. 2000; Motta and Nola 2001), and increased tree establishment (e.g. Körner 2003; Daly and Shankman 1985). Many mountain regions such as the European and Swiss Alps have experienced simultaneous changes in both land use and climate, thus it can be difficult to identify the specific causes of these vegetation changes (see discussions by Beniston et al. 1997 and Gehrig-Fasel et al. 2007).

In North America, the boreal tree line has received far more attention in terms of paleoclimatological and paleoecological research than the alpine tree line (e.g. Kerwin et al. 2004; MacDonald et al. 1993). In the Rocky Mountain region in north-central Colorado, however, significant changes in both climate and land use/land cover have and are occurring. Kittel et al. (2007) found that over the period 1953–2006, the mean maximum air temperature in the subalpine forest site near that used in this study increased for much of the year at a rate of +0.4°C per decade, yet there was no trend in precipitation changes. Near the alpine site used in this study, Kittel et al. (2007) found (over the same period) a decrease in the mean maximum air temperatures in winter (−0.4 to −0.6°C per decade), and an increase in October through April precipitation (+100 mm per decade). Natural fire occurrence (Sherriff et al. 2001), together with logging and mining have all, at times, affected forest cover (e.g. Baker et al. 2007), and the recent mountain pine beetle outbreak will drastically alter the landscape within the next decade (Negron and Popp 2004). In addition, the study area along the continental divide is adjacent to one of the faster growing population regions in the United States, thus the deposition of pollutants with the upslope easterly winds can impact ecosystem functions (e.g. Sievering et al. 2007).

There have been few observations of exchanges of energy, water and carbon in complex mountainous terrain, despite the significance of such regions as described above. Studies conducted at the subalpine forest site that is used in this study have shown that eddy-covariance can be a reliable method in complex terrain (Turnipseed et al. 2002), and that horizontal advection of CO_2 at that site can be significant during periods of low turbulent mixing (Sun et al. 2007; Yi et al. 2008). In alpine tundra near the alpine study site, Cline (1997) showed that the aerodynamic profile method could be used to give reliable estimates of the surface energy balance, and other short-term eddy-covariance studies conducted in steep, complex terrain have shown that quality measurements can be made (e.g. Gu et al. 2008; Lewicki et al. 2008; Hammerle et al. 2007).

We present observations of water and carbon dioxide exchange above high-altitude alpine tundra near Niwot Ridge, Colorado, USA, and compare and contrast the alpine measurements to simultaneous measurements conducted over an adjacent subalpine forest, over a period spanning two summers and one winter. After first discussing the quality of the eddy-covariance based measurements, we then compare

the general meteorological and surface flux measurements between sites. Despite large differences in above-ground biomass, surprising similarities and differences were found in the diurnal and seasonal water and carbon exchanges.

Materials and methods

The eddy covariance method was used to measure turbulent fluxes of water (latent heat flux, λE), heat (sensible heat flux, H), and CO_2 (F_C) over a period from June 9, 2007 through July 3, 2008. Pertinent details describing the alpine tundra site and subalpine forest site are presented below.

Alpine tundra site

The alpine study site is located above tree line at an elevation of 3,480 m above sea level (40°03′11″N; 105°35′11″W) on a flat ridge top (Niwot Ridge, Colorado). To our knowledge, this is the highest-elevation eddy covariance site in the world, exceeding the elevation of flux measurements made on the Tibetan Plateau (3,250 m; Gu et al. 2008). The site is considered an alpine fellfield, one of the most widespread Front Range alpine communities (Walker et al. 2001), and is characterized by high wind speeds, dry soils, low snow accumulation, and sparse vegetation cover. Vegetation is short (less than 5 cm tall) with a leaf area index, *LAI,* less than 0.5 m^2 m^{-2}, and is dominated by *Carex rupestris* (curly sedge), *Kobresia myosuroides* (Bellardi bog sedge) with a high root: shoot ratio (Humphries et al. 1996), and *Paronychia pulvinata* (Rocky Mountain nailwort) (Walker et al. 2001). Long-term (1981–2008) continuous climate data collected at the nearby Saddle site indicate a mean annual air temperature of −2.15°C and 966 mm total annual precipitation.

A pair of identical eddy covariance systems were located 50 m apart along an east-west axis (parallel to the prevailing wind direction: Fig. 1). A sonic anemometer (CSAT 3, Campbell Scientific) and open-path gas analyzer (LI-7500, LI-COR) were mounted 3 m above the ground facing north. Additional instrumentation mounted at 3 m included air temperature and humidity (shielded HMP 45C, Vaisala), and net radiation (R_n; NR-Lite, Kipp and Zonen). The soil heat flux (G) was measured at each site using a pair of soil heat flux plates buried at a depth of 2 cm (HFT3, REBS). Half-hour statistics from data sampled at 10 Hz (sonic and gas analyzer) and 5 s (all other sensors) were calculated using a datalogger (CR3000, Campbell Scientific). All raw data were transmitted in real-time via radio (900 MHz Spread Spectrum, FreeWave) and archived by the Niwot Ridge LTER program at INSTAAR at the University of Colorado in Boulder. 120-V AC power was available at both sites. Post-processing of the eddy covariance data to calculate the turbulent fluxes included all of the standard corrections and adjustments (e.g. coordinate rotation, Webb adjustment, etc.) following Aubinet et al. (2000) and Lee et al. (2004), similar to those corrections for the subalpine site on Niwot Ridge.

In complex terrain that may be especially prone to katabatic cold-air drainage, the vertical turbulent flux of CO_2 as measured using the eddy covariance method (F_C; $u$mol m^{-2} s^{-1}) may not equal the net ecosystem exchange (*NEE*) during periods of low wind speeds due to changes in the time rate of change of CO_2 concentration beneath the sensor height (F_S; $u$mol m^{-2} s^{-1}), and the horizontal advection of CO_2 (F_H; $u$mol m^{-2} s^{-1}). Horizontal advection, in fact, has been reported in relatively flat sites during calm conditions associated with noctural drainage flows (e.g. Aubinet et al. 2003; Leuning et al. 2008). Therefore, we approximate the alpine *NEE* as:

$$\begin{aligned} NEE &= F_C + F_S + F_H \\ &= \frac{1}{V_m}\overline{w'c'}(z_r) \\ &\quad + \int_0^{z_r}\left[\frac{1}{V_m}\frac{\partial \overline{c}(z_r)}{\partial t} + \frac{1}{V_m}\overline{u}(z_r)\frac{\partial \overline{c}(z_r)}{\partial x}\right]\mathrm{d}z \end{aligned} \quad (1)$$

where V_m is the molar volume of dry air (m^3 mol^{-1}), w is the vertical wind component (m s^{-1}), c is the molar fraction of CO_2 ($u$mol mol^{-1}) measured at the reference height $z_r = 3$ m, primes note deviations from the 0.5 h means, t is time (seconds), and $\overline{u}(z_r)$ is the component of the mean horizontal wind speed (m s^{-1}) aligned with the horizontal ($\Delta x = 50$ m) CO_2 concentration gradient. In practice, we used finite differences to approximate the spatial derivatives in Eq. 1, and used one-level measurements at z_r to approximate the integrals due to the low measurement height, sparse canopy, and windy conditions, coupled with the uncertainty of evaluating vertical profiles as described next.

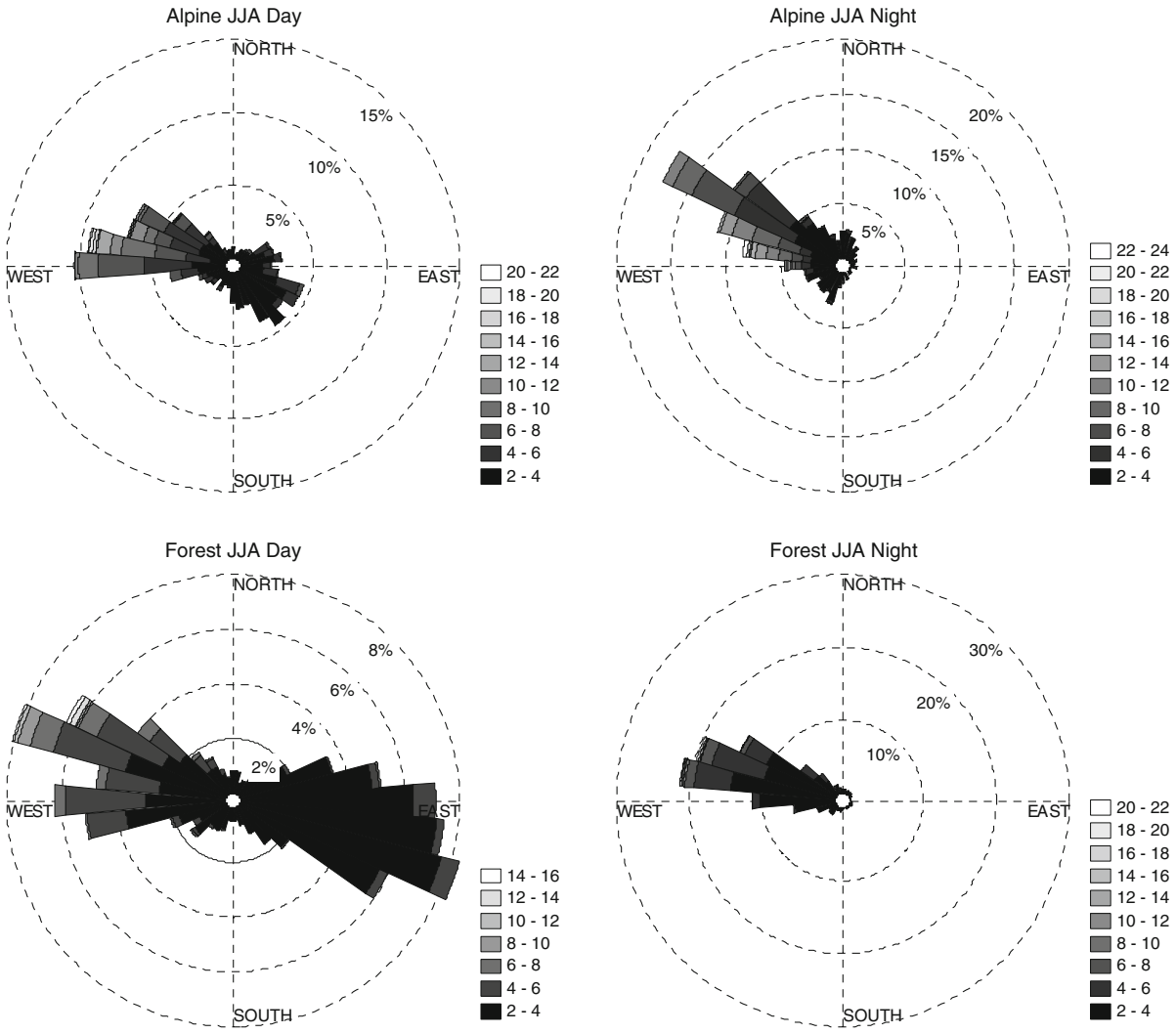

Fig. 1 Frequency of wind by direction and speed (ms^{-1}) during the summer months (June-July-August) for the alpine (*top panels*) and forest (*bottom panels*) sites during daytime (*left panels*; 8 am–4 pm), and nighttime (*right panels*; 8 pm–4 am) periods

Even with technically demanding and expensive experiments specifically designed to measure horizontal and vertical advection, Leuning et al. (2008) has shown that the spatial and temporal variations in vertical wind velocities and horizontal concentration gradients make the measurements of the advection terms so difficult that they can not be calculated to the required accuracy. In this study, using sonic anemometers with a vertical wind speed resolution of 0.5 mm s^{-1}, gas analyzers with a RMS of 0.0043 mmol m^{-3}, and a horizontal separation distance of 50 m (similar to the separation used in other studies such as Feigenwinter et al. 2008; Leuning et al. 2008), the uncertainly in the estimate of F_H at night was large (standard deviations of 0.0427 and 0.0736 *u*mol m^{-2} s^{-1}, summer and winter nights, respectively), relative to the means shown in Table 1. This implies that even when trying to account for flows not aligned with the two towers (Kutsch et al. 2008), there still were difficulties in measuring F_H due to the sensitivity of F_H to errors in measurements of wind vectors and horizontal concentration gradients.

As described in the Results and Discussion section, use of the double coordinate rotation method (or planar fit method) forced vertical advection to zero, hence vertical advection was not explicitly included in Eq. 1 because vertical profiles of CO_2 concentrations

Table 1 Mean values of alpine *NEE*, eddy-covariance turbulent flux (F_C), horizontal advection flux (F_H), and the storage flux (F_S) measured during the daytime (8 am–4 pm MDT) and nighttime (8 pm–4 am MDT), summer (JJA) and winter (DJF)

	Summer		Winter	
	Daytime	Nighttime	Daytime	Nighttime
NEE	−1.66	1.05	1.67	1.49
F_C	−1.73	0.992	1.67	1.47
F_H (F_H/NEE)	0.0745 (5)	0.0667 (6)	0.00630 (<1)	0.0136 (<1)
F_S (F_S/NEE)	−0.00290 (<1)	−0.00170 (<1)	−0.00310 (<1)	0.0030 (<1)

All values are in μmol m^{-2} s^{-1} except for ratios (%)

were not measured. Some studies, however, have reported that vertical advection is of similar magnitude but opposite sign to F_H (e.g. Aubinet et al. 2003; Feigenwinter et al. 2004; Sun et al. 2007; Wang et al. 2005), and therefore recommend to include neither or both in CO_2 budget studies. In this study, persistent high wind speeds and associated turbulent mixing coincided with a small F_H relative to F_C, so including only the one advective term could be erroneous, but nonetheless has been included to show the potential magnitude of the adjective terms.

At the alpine site, the wind direction was nearly exclusively from the west in close alignment with the orientation of the two towers. Wind roses (Figs. 1 and 2) show that upslope (easterly) winds were fairly common during the daytime in the summer at the forest site yet seldom reached the alpine site. Downslope (westerly) winds prevailed at both sites at night during the summer, and both day and night during the winter. Following the approach described in Kutsch et al. (2008), horizontal advection could also occur in mixed situations of wind and slope-aligned katabatic drainage flows, and therefore a wind vector proportional to the gradient-based alignment of the towers to account for winds not perfectly aligned with the two towers was calculated. Although multiple sampling locations, hence towers, are ideal to quantify both F_S and F_H (e.g. Fegenwinter et al. 2008; Sun et al. 2007), only measurements at two locations were available to estimate F_S and F_H as has been the case in several studies (e.g. Aubinet et al. 2003; Staebler and Fitzjarrald 2004; Sun and Mahrt 1994; Wang et al. 2005).

Accounting for the recently recognized potential effects of additional sensible heat exchange from the top, bottom, and spars of the open-path gas analyzer on the alpine F_C measurements (Burba et al. 2008 using their "Method 4"), on average a 6% reduction in F_C over the entire measurement period, similar to the magnitude of the horizontal advection term, was found. Although not particularly significant on a short-term (i.e. diurnal) basis, this new correction could be significant when looking at long-term (i.e. annual) carbon budgets, thus this correction warrants further investigation and the application of this correction should be treated with caution (Burba et al. 2008).

Subalpine forest site

The subalpine forest site was located roughly 4 km east of the alpine site, at an elevation of 3050 m above sea level (40°01′58″N; 105°32′47″W) on a ~5% east-sloping surface. The site is considered a low-productivity subalpine forest, and is dominated by *Picea engelmannii* (Engelmann spruce), *Abies lasiocarpa* (subalpine fir), *Pinus flexilis* (limber pine), and *Pinus controrta* (lodgepole pine) with a mean height of 11.5 m and an *LAI* of 4.2 m^2 m^{-2} (Monson et al. 2002; Turnipseed et al. 2002, 2003). Conditions are warmer and drier than the alpine site, with a long-term (1952-present) mean annual air temperature of 1.5°C and 800 mm annual precipitation.

Instrumentation at this site is fully described in other papers (e.g. Turnipseed et al. 2002, 2003). Briefly, eddy covariance instruments were mounted 21.5 m above the ground from a 26 m tall scaffolding tower. Several instruments (e.g. sonic anemometers, open and closed-path gas analyzers, net radiometers) were located at the site, with intercomparisons presented in Turnipseed et al. (2002). Both local-scale and meso-scale effects that influence airflow and turbulent flux measurements are described in Turnipseed et al. (2003) and Turnipseed et al. (2004), respectively, and a detailed investigation of the role of

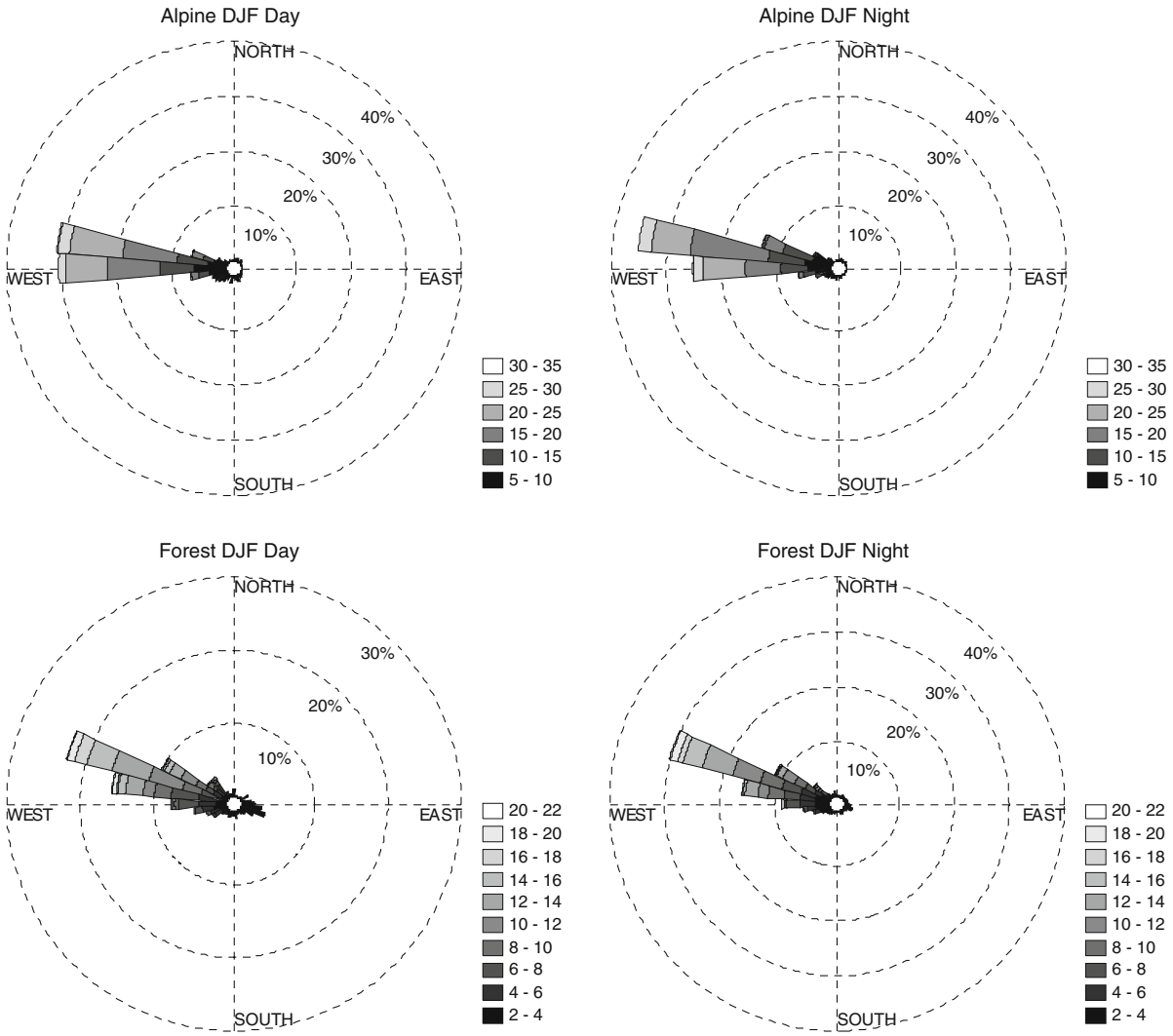

Fig. 2 Frequency of wind by direction and speed (ms^{-1}) during the winter months (December-January-February) for the alpine (*top panels*) and forest (*bottom panels*) sites during daytime (*left panels*; 8 am–4 pm), and nighttime (*right panels*; 8 pm–4 am) periods

advection in net ecosystem exchange is presented in Sun et al. (2007) and Yi et al. (2008). The influences of snowpack on soil respiration are described by Monson et al. (2002, 2006) and Bowling et al. (2009).

Results and discussion

Assessments of data quality

Although short-term turbulent flux measurements have been made near the alpine site in the past (e.g. Cline 1997), the focus of that study was on the snowmelt period, and CO_2 fluxes were not measured. In addition, fluxes were calculated based on aerodynamic formulae (i.e. profiles) requiring empirical atmospheric stability corrections. Improvements in both our understanding of micrometeorology in complex terrain (e.g. Hammerle et al. 2007) and advances in instrumentation (e.g. fast-response sensors) have increased the quality of turbulent flux measurements in complex terrain. A key assessment of the quality of flux measurements is surface energy balance closure; the degree to which the non-turbulent terms (available energy: R_n-G) balance the turbulent terms (λE and H). Figure 3 shows an

example of surface energy balance closure at the alpine site during the summer (JJA) and winter (DJF) months. Based on the slope of the linear regression lines, $\lambda E + H$ was within 9% of R_n-G indicating a closure of 91% during the summer months, and within 29% (closure of 71%) during the winter months with an expected decrease in winter-time closure due to a marked decrease in the magnitude of the turbulent fluxes (see Fig. 10). This degree of the summer-time surface energy balance closure is comparable to that observed at the forest site on Niwot Ridge (84%; Turnipseed et al. 2002), and overall similar or improved compared to other high-latitude alpine sites (e.g. 70%; Gu et al. 2008), and sites located in steep, complex terrain (e.g. 77%; Lewicki et al. 2008: 72%; Hammerle et al. 2007). Also, since the alpine site was located on a relatively flat yet high-altitude ridge, the rotation transform angle for the sonic anemometer in the horizontal-vertical plane varied only by roughly 5 degrees depending on wind direction regardless of season, with outliers associated with low wind speeds (Fig. 4). In addition to the double rotation method that was applied to the alpine flux data (the mean cross-wind and vertical-wind velocity components were rotated to zero for each 0.5 h; McMillen 1988) the planar fit method, thought to be preferable in complex terrain (Wilczak et al. 2001), was also applied. Using the planar fit method resulted in similar rotations angles (e.g. 3.6° in the horizontal-

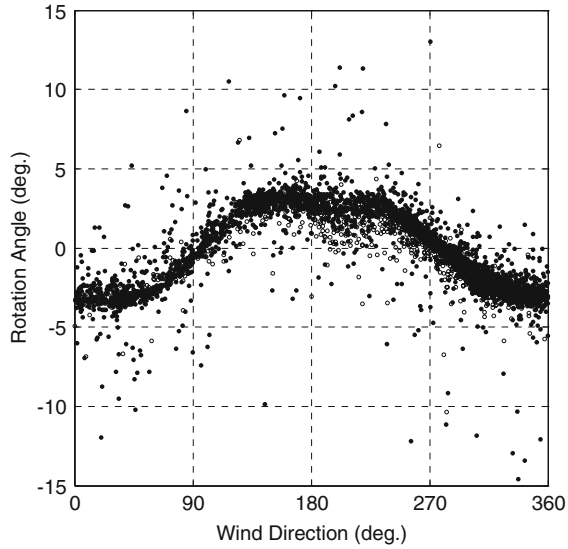

Fig. 4 The rotation transform angle for the sonic anemometer in the horizontal-vertical plane for summer (*filled circles*: June-July-August) and winter (*open circles*: December-January-February)

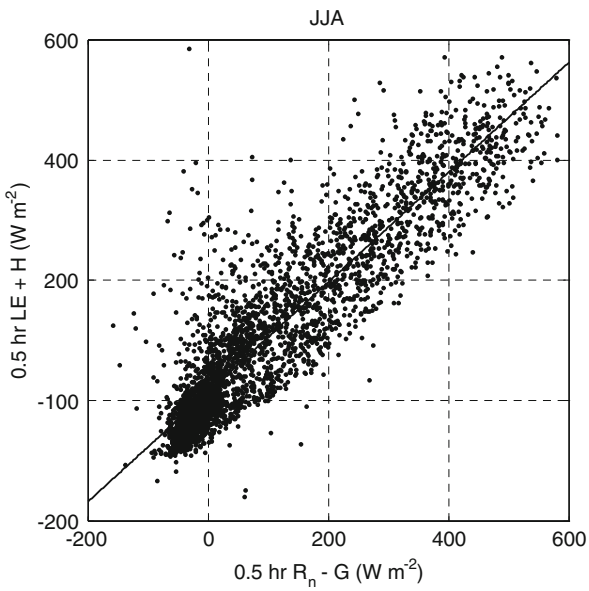

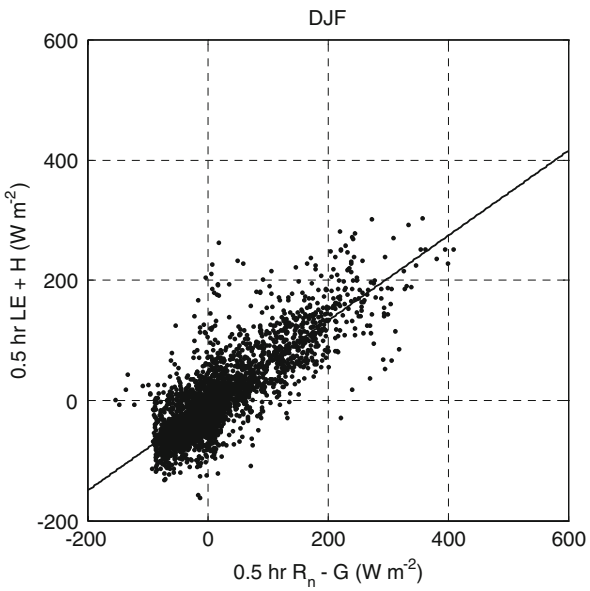

Fig. 3 Alpine 0.5 h mean available energy (net radiation minus the soil heat flux) versus the sum of the latent and sensible heat fluxes for summer (June-July-August) and winter (December-January-February) months. Equation of the linear regressions (*lines*) are summer: $y = 0.91x + 16$ W m^{-2} ($r^2 = 0.83$; $n = 4{,}000$), and winter: $y = 0.71x - 7$ W m^{-2} ($r^2 = 0.66$; $n = 4{,}318$)

vertical plane), and therefore there was no significant affect of rotation method on the turbulent flux calculations.

The high quality of the turbulent flux measurements was also largely due to the relatively short flux footprint, calculated using the analytical solution to the diffusion equation as described by Schuepp et al. (1990). During all conditions (typical daytime, nighttime, and neutral atmospheric stability), the upwind distance that the turbulent fluxes measurements were most sensitive to occurred within 40–50 m of the tower (Fig. 5a). The cumulative footprint (Fig. 5b) shows that 80% of the turbulent fluxes originated from distances of 340, 381, and 368 m during typical daytime, nighttime, and neutral atmospheric stability conditions, respectively. The similarity in the footprint calculations for both daytime and nighttime conditions compared to neutral atmospheric stability conditions was indicative of the persistent windy, near-neutral stability conditions.

The relatively short turbulent flux footprints relative to the scale of the spatial heterogeneity, ridge-top site location, and lack of strong sources or sinks of CO_2 in the sparse tundra vegetation upwind of the alpine site coupled with high horizontal wind speed and friction velocity (u_*) combined to result in a small F_S and F_H relative to F_C. Several studies (all conducted in forests) have demonstrated that F_S and F_H tended to be large at night when u_* was low, and hence many have used a u_* filter (threshold) to replace F_C values at low u_* with some form of soil or air temperature-based estimate of respiration, thus avoiding the advection issue (e.g. Goulden et al. 1996). Figure 6a shows that the nighttime alpine F_C showed only a weak dependence on u_*, only below roughly 0.15 m s^{-1}, slightly less than the u_* threshold of 0.20 m s^{-1} determined at the forest site used in this study (Monson et al. 2002). The windy, turbulent conditions experienced at the alpine site resulted in relatively few low u_* conditions even at night (Fig. 6d). Over the entire study period, u_* was less than 0.15 m s^{-1} only 10% of the time, thus rejecting F_C at $u_* < 0.15$ m s^{-1} had no significant effect on our estimate of *NEE* (see Fig. 14).

Both F_H and F_S showed similar behavior with u_* to that reported in other studies at forested sites; F_H decreased as u_* increased (Fig. 6b), and F_S increased until u_* reached $\sim$0.4 m s^{-1} and subsequently decreased (Fig. 6c). The increase in F_S until $\sim$0.4 m s^{-1} occurred because a minimum amount of turbulence was required to evacuate any CO_2 accumulation beneath the sensor height. As u_*

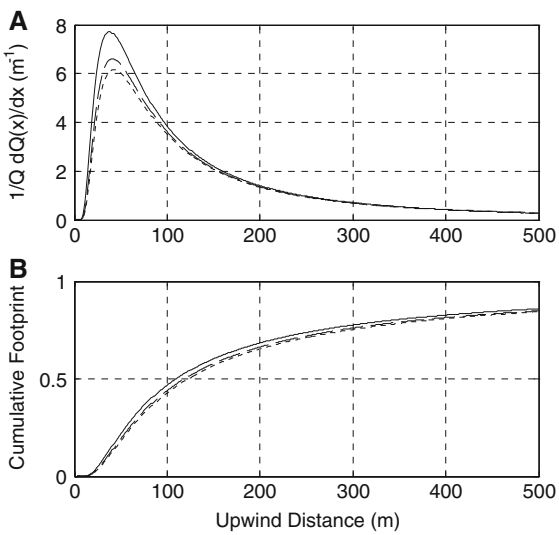

Fig. 5 Turbulent flux footprints showing the upwind distance that the flux measurements were most sensitive to (**a**) and the cumulative footprint showing how much of the flux originated with upwind distance (**b**), for typical daytime (*solid*), nighttime (*dotted*) and neutral (*dashed*) atmospheric stability conditions

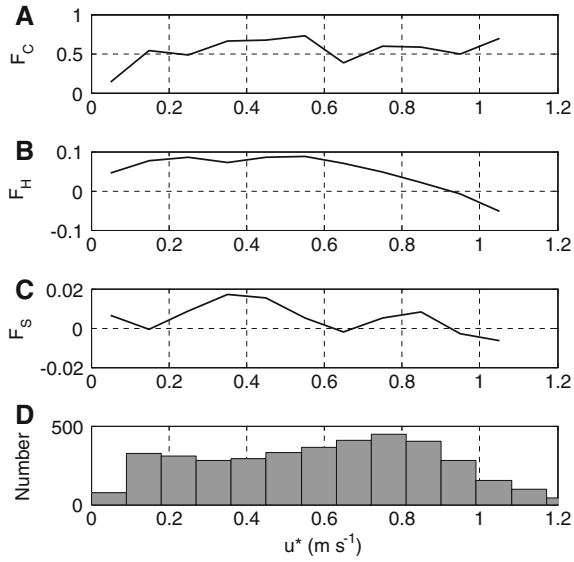

Fig. 6 A: Eddy-covariance measured turbulent flux (**a**: F_C), horizontal advection flux (**b**: F_H), and storage flux (**c**: F_S) during the night (8 pm–4 am MDT) shown as means corresponding to friction velocity bin classes of 0.1 m s^{-1}. Histogram (**d**) shows the distribution of the nocturnal friction velocity

increased, the horizontal advection of CO_2 beneath the sensor height decreased as turbulent mixing displaced the cold, dense low-lying air, or decreased as turbulent mixing reduced the horizontal gradients of CO_2.

An example of the diurnal behaviors of F_C, F_H, and F_S during a 5 day summer period shows that F_H tended to be large relative to F_C at night, then decreased but remain positive during the daytime (Fig. 7). F_S tended to be small relative to F_C except for a few brief periods at sunrise. Averaged over summer and winter months, F_H varied from less than 1% (winter) to a maximum 5–6% (summer) of *NEE* (Table 1). When averaged over daytime and nighttime periods, F_S was small due to the high wind speeds and relatively low measurement height.

Comparison of meteorological conditions

The seasonal trend in air temperature (T_a) and relative humidity were similar between sites (Fig. 8a, b) indicative of the same synoptic-scale air mass influences. The mean T_a at the alpine site, however, was roughly 2°C lower than the forest during the summer (Table 2), and nearly 3°C lower during the winter (Table 3). Following the dry adiabatic lapse rate of 1°C per 100 m, the decrease in T_a due to the 430 m change in elevation was 4.30°C (or an estimated 2.15°C with a minimum moist adiabatic lapse rate of 0.5°C per 100 m), so differences in T_a could be due to differences in vegetation cover.

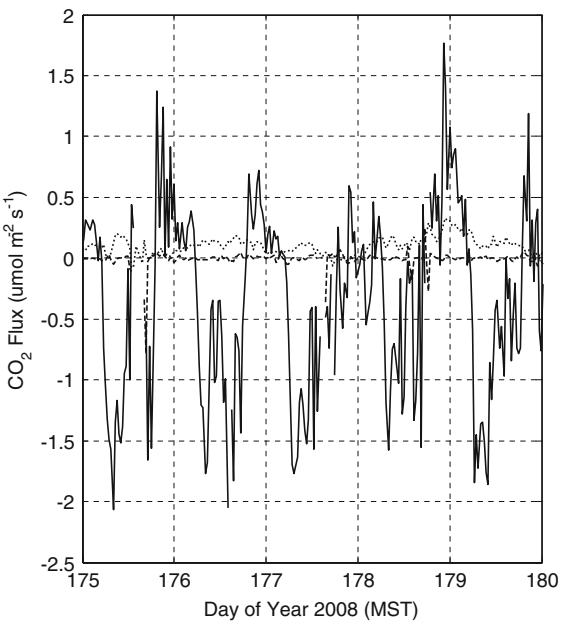

Fig. 7 Diurnal example of the magnitudes of the eddy-covariance measured turbulent flux (F_C; *solid line*), horizontal advection flux (F_H; *dotted line*), and storage flux (F_S; *dashed line*) at the alpine site

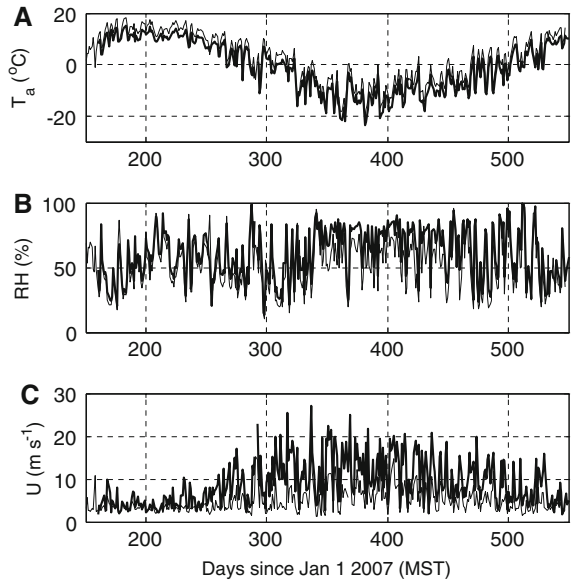

Fig. 8 24 h mean air temperature (**a**), relative humidity (**b**), and horizontal wind speed (**c**) measured at the alpine (*thick line*) and forest (*thin line*) sites

Air temperature at the alpine site was measured 3 m above the ground, compared to 21 m above the ground, 9.6 m above the 11.4 m-tall canopy at the forest site. The effect of the forest vegetation canopy on T_a was evident when comparing T_a measured below the forest canopy, but at similar height above the ground (2 m) compared to the 3 m alpine measurement height (Fig. 9a). Compared to the alpine and above-canopy forest T_a, the beneath-canopy T_a values were higher during the daytime (downward sensible heat from the canopy) and lower at night (sub-canopy katabatic drainage flows; Fig. 1). While following similar annual trends (Fig. 8b), differences in relative humidity between sites were more pronounced in the winter than summer (Tables 2 and 3) due to the lower T_a at the alpine site and non-linear saturation vapor pressure-temperature relationship.

The most characteristic meteorological variable of the alpine/subalpine forest and most noticeable difference between sites was the high horizontal

Table 2 Summer (June–July–August) mean 0.5 h conditions observed at the alpine and forest sites, 24 h, daytime (8 am–4 pm), and nighttime (8 pm–4 am) periods

	24 h		Daytime		Nighttime	
	Alpine	Forest	Alpine	Forest	Alpine	Forest
Air temperature (°C)	10.98	13.09	12.72	15.11	9.52	11.36
Relative humidity (%)	54.18	51.32	50.72	47.03	57.65	55.06
Horizontal wind speed (m s^{-1})	4.44	3.31	4.41	3.28	4.45	3.48
Net radiation (W m^{-2})	91.25	155.03	313.34	460.29	−64.03	−60.24
Sensible heat flux (W m^{-2})	32.37	47.77	121.05	187.77	−26.54	−42.91
Latent heat flux (W m^{-2})	58.72	77.03	138.07	161.66	4.02	13.02
Soil heat flux (W m^{-2})	9.55	3.39	79.10	14.49	−38.19	−4.48

Table 3 Winter (December–January–February) mean 0.5 h conditions observed at the alpine and forest sites, 24 h, daytime (8 am–4 pm), and nighttime (8 pm–4 am) periods

	24 h		Daytime		Nighttime	
	Alpine	Forest	Alpine	Forest	Alpine	Forest
Air temperature (°C)	−12.24	−8.69	−11.56	−7.71	−12.67	−9.26
Relative humidity (%)	73.38	60.46	72.10	56.96	74.26	62.86
Horizontal wind speed (m s^{-1})	13.21	7.13	13.14	7.23	13.47	7.06
Net radiation (W m^{-2})	3.52	42.80	81.05	208.74	−37.56	−43.69
Sensible heat flux (W m^{-2})	−4.62	9.61	33.79	121.52	−25.97	−50.47
Latent heat flux (W m^{-2})	7.17	38.14	21.10	58.02	−0.09	27.40
Soil heat flux (W m^{-2})	−8.85	−2.02	7.73	−2.03	−17.45	−2.01

wind speed (U). At both sites, U increased in the winter periods, corresponding closely to the period when T_a decreased below 0°C (Fig. 8c), and air was flowing downslope at both sites (Fig. 2). The average winter U exceeded 13 m s^{-1} at the alpine site during the night and day, roughly double that observed above the canopy at the forest site (Table 3), yet the average U during the summer was much lower and more similar between sites (Table 2). As described above, this persistent strong downslope wind at the alpine site helped to moderated horizontal advection of CO_2 at the alpine site.

Comparison of the surface energy balance

The differences in vegetation (trees versus tundra) coupled with the cooler, slightly more humid, and windier conditions at the alpine compared to the forest site was apparent in all components of the surface energy balance. For example, R_n was always greater at the forest compared to the alpine site, presumably due to a lower albedo (Figs. 10a and 11a). The mean daytime R_n at the two sites were more similar in the winter months (128 W m^{-2}; Table 3) compared to the summer months (147 W m^{-2}; Table 2) indicating that vegetation, not seasonal changes in snow cover, played a major role in seasonal differences in R_n between sites.

The sensible heat flux (H) was generally small with similar patterns at both sites for most of the measurement period except for early winter (Figs. 10b and 11b). In the early winter, H from the forest could exceed 100 W m^{-2} (24 h average) compared to an early-winter negative (downward) H at the alpine site. During the early-winter period, the forest canopy was relatively warm compared to the ambient air temperature, whereas the alpine tundra was relatively cold compared to the ambient air temperature. Seasonal differences in the latent heat flux (λE) between sites were also more apparent

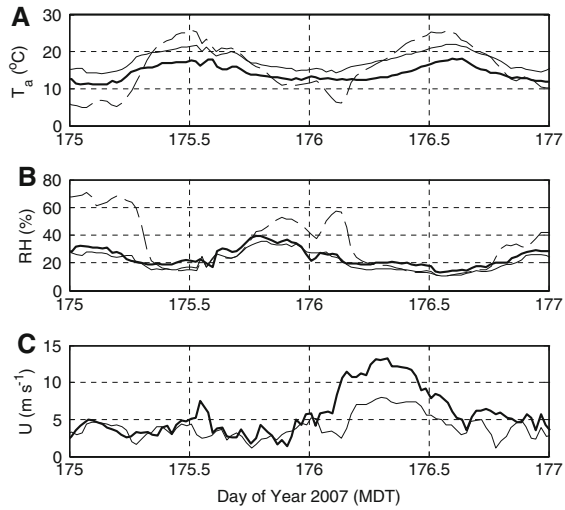

Fig. 9 Sample 0.5 h mean air temperature (**a**), relative humidity (**b**), and horizontal wind speed (**c**) measured at the alpine (*thick lines*), and above-forest (21 m: *thin lines*) and below-forest canopy (2 m: *dashed lines*) sites (June 24th and 25th)

during the winter period (Fig. 10c) compared to the summer periods (e.g. Fig. 11c). Although the contribution to λE from transpiration can not be isolated, the summertime forest λE exceeded that from the alpine likely due to greater transpiration from the forest. During the winter, the larger λE from the forest site was likely due to the added contribution to λE from the sublimation of intercepted and beneath-canopy snow Molotch et al. (2007), since transpiration should be negligible at that time of year. The seasonal change in the partitioning of R_n between H and λE (the evaporative fraction; $\lambda E/(H + \lambda E)$) was similar at the two sites, despite the large difference in above-ground biomass. The soil heat flux, however, was markedly different (Figs. 10d and 11d), with a much higher G at the alpine site due to the lack of vegetation cover and higher fraction of exposed bare ground, and lack of continuous snow cover in the winter months.

Comparison of net ecosystem exchange of CO_2

Figure 12a shows that the 24 h mean *NEE* at both sites was most similar during the winter season. The forest site continued a net daytime CO_2 uptake (negative *NEE*) much longer into the fall and switch to net CO_2 uptake much earlier in the spring (Fig. 12b). Nighttime *NEE* (respiration) was larger

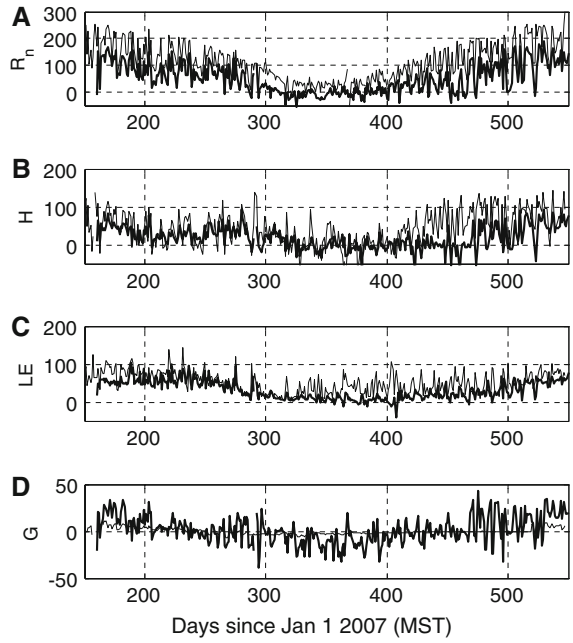

Fig. 10 24 h mean surface energy balance components for the alpine (*think lines*) and forest (*thin lines*) sites: net radiation (**a**), sensible heat flux (**b**), latent heat flux (**c**), and soil heat flux (**d**), all in W m^{-2}

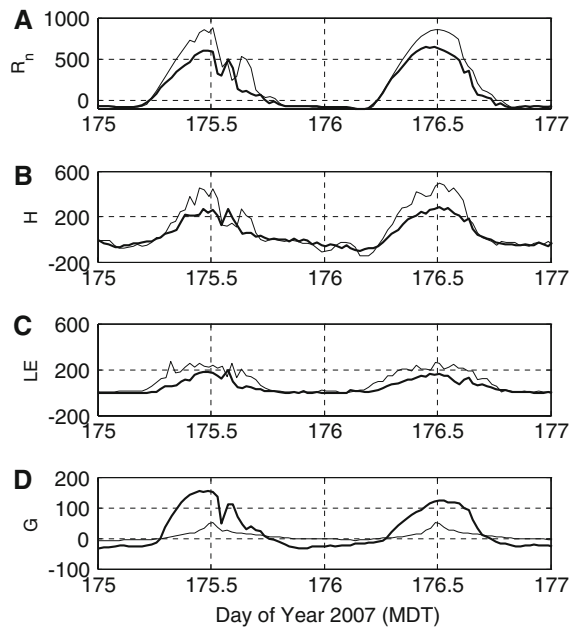

Fig. 11 0.5 h mean surface energy balance components for the alpine (*thick lines*) and forest (*thin lines*) sites: net radiation (**a**), sensible heat flux (**b**), latent heat flux (**c**), and soil heat flux (**d**), all in W m^{-2}, for June 24 and 25, 2007

from the forest site in the summer (Fig. 12c). At both sites, the switch from positive *NEE* (respiration) to negative *NEE* (assimilation) corresponded to changes in T_a to +10°C (Table 4). An example of a typical diurnal pattern of *NEE* at the two sites (Fig. 13) further illustrates the larger uptake and release of CO_2 by the forest compared to the alpine site. The differences, however, in the diurnal *NEE* patterns were not as large as initially expected given the difference in *LAI* at the two sites, since others have reported strong correlations between *LAI* and *NEE* (e.g. Jarlan et al. 2008; Shi et al. 2006).

One of the most valued benefits of using the eddy covariance method to continuously measure carbon and water cycling is the ability to estimate the annual carbon and water budgets. As has been discussed, however, *NEE* estimates based on eddy covariance measurements need to directly account for horizontal advection and storage of CO_2 (e.g. Eq. 1), or alternatively, use a u_* filter to replace F_C measurement below a u_* threshold with temperature-based estimates of nocturnal respiration. In Fig. 14, three estimates of the long-term *NEE* measured at the alpine site are shown; the vertical turbulent flux (F_C), F_C with F_C values when $u_* < 0.15$ m s^{-1} (Fig. 6a) were replaced with an estimate of respiration based on the empirical relationship of F_C versus air temperature ($r^2 = 0.70$; not shown), and *NEE* calculated using Eq. 1. Figure 14 shows that the use of the

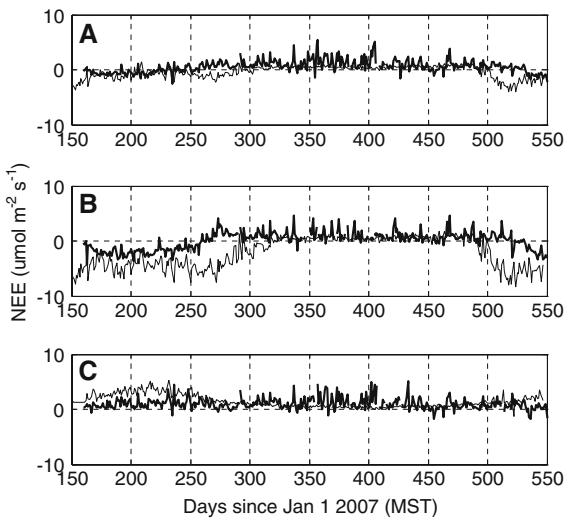

Fig. 12 Mean net ecosystem exchange of CO_2 ($u$mol m^{-2} s^{-1}) at the alpine (*thick lines*) and forest (*thin lines*) sites for 24 h (**a**), daytime (**b**) and nighttime (**c**) periods

u_* filter tended to give consistently higher estimates of the cumulative C exchange compared to the other two methods. F_C tended to be lowest of the three estimates, especially during periods of net uptake, and *NEE* calculated with F_H and F_S was somewhere between the other two estimates. At the end of the measurement period, however, all three methods were similar (153.7 163.6, 163.8 g C m^{-2}, F_C, F_C with u_* filter, and Eq. 1, respectively), and all indicated that the alpine site was a net source of C when integrated over two summers and one winter.

Since the three estimates of the cumulative C balance at the alpine site were quite similar, Fig. 15 compares the alpine *NEE* using Eq. 1 to the forest's *NEE*, and compares both to the cumulative atmospheric water exchange (E). Over the course of the entire measurement period, the alpine site had a net loss of both carbon and evaporative water, whereas the forest site had a net carbon gain coupled with an evaporative water loss greater than the alpine site.

Comparing *NEE* and E over the two complete periods with a net C gain to the surface ($NEE > 0$) and a net C loss from the surface ($NEE < 0$), interesting differences emerged (Table 4). The start of the alpine net C uptake period was delayed by 44 days compared to the forest site, and at both sites the start date coincided with the date when T_a reached +10°C. The summer period of alpine net C uptake ended 64 days before the forest site (therefore the period of C uptake was 100 days for the alpine site compared to 208 days at the forest site), and the end of this period coincided with the date when T_a decreased below −10°C. The ecosystem water use efficiency of the two sites, calculated as the ratio of the total C gain to the total H_2O loss (and recognizing that this represents the surface as a whole since not 100% of H_2O was transpired) was 0.25 g C/kg H_2O at the forest compared to 0.08 g C/kg H_2O the alpine site. Comparing the ecosystem water use efficiencies shows that the forest was more than three-times more efficient than the alpine tundra.

The switch to net C loss at both sites coincided with the date when T_a decreased below −10°C (Table 4), which occurred earlier in the year at the alpine site. Net C loss ended when T_a increased above 0°C at both sites, and since this occurred earlier in the year at the forest site, the overall length of the net C loss period was 96 days longer at the alpine site. The net C loss was more than three-times that from the

Table 4 Summary of conditions for the periods with consecutive days of daily-averaged negative *NEE* (net CO_2 uptake by the surface) and positive *NEE* (net loss of CO_2 from the surface)

	Start date (DOY)	Start date T_a (°C)	End date (DOY)	End date T_a (°C)	Period length (days)	$\sum_{start}^{end} C$ ($g\ m^{-2}$)	$\sum_{start}^{end} H_2O$ (mm)	$\frac{\sum_{start}^{end} C}{\sum_{start}^{end} H_2O}$ ($g\ C/kg\ H_2O$)
Alpine NEE < 0	June 9, 2007 (160)	Reaches +10	Sept 17, 2007 (260)	Falls below −10	100	16 net gain	196 net loss	0.08
Forest NEE < 0	April 26, 2007 (116)	Increases from −10 to +10	Nov 20, 2007 (324)	Falls below −10	208	108 net gain	432 net loss	0.25
Alpine NEE > 0	Sept 18, 2007 (261)	Falls below −10	June 16, 2008 (167)	Increases above 0	271	164 net loss	186 net loss	−0.88
Forest NEE > 0	Nov 21, 2007 (325)	Falls below −10	May 14, 2008 (135)	Increases from −10 to nearly +10	175	52 net loss	228 net loss	−0.23

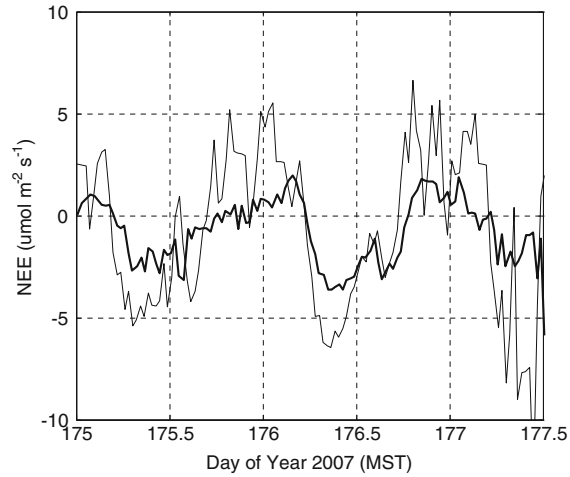

Fig. 13 0.5 h mean *NEE* at the alpine (*thick line*) and forest (*thin line*) sites (June 24th and 25th)

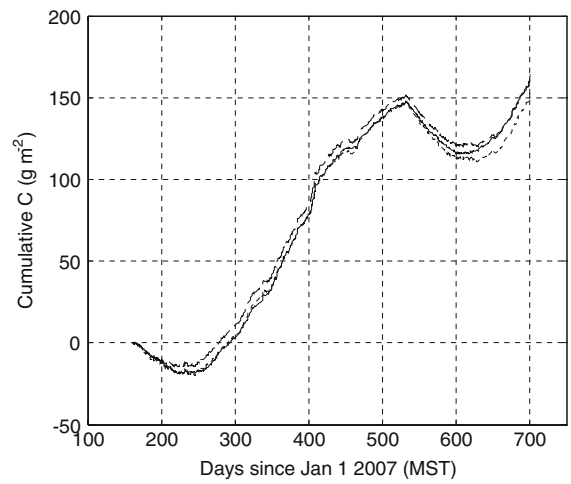

Fig. 14 Cumulative carbon balance at the alpine site based on three estimates of *NEE*: F_C alone (*dotted line*), F_C with a u_* filter (*dashed line*), and $F_C + F_H + F_S$ (*solid line*). Values at the end of the measurement period were 153.7, 163.6, and 163.8 g C m^{-2}, F_C, $F_C + F_H + F_S$, and F_C with u_* filter, respectively

forest, and coupled with similar H_2O losses, the resulting ratio of C loss to water loss was nearly four-times greater at the alpine site.

Conclusions

The first results from, to the authors' knowledge, the highest elevation alpine tundra eddy covariance site

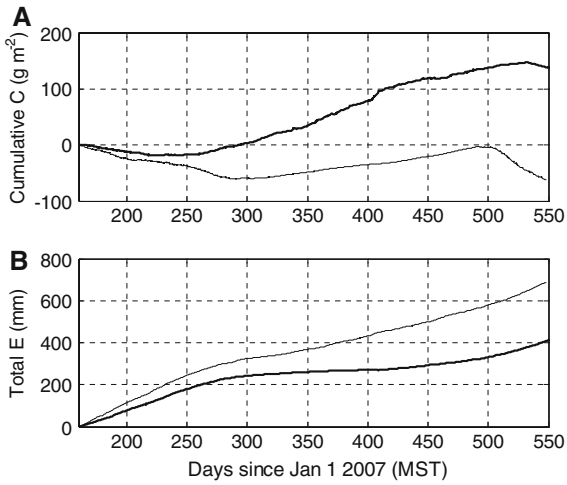

Fig. 15 Cumulative *NEE* expressed in g m^{-2} of carbon (**a**) and total evaporative water loss (**b**) for the alpine (*thick lines*) and forest (*thin lines*) sites over matching periods. Values at the end of the measurement period were 139 and −62 g C m^{-2}, 408 and 688 mm H_2O, alpine and forest, respectively

in the world, were presented and compared to simultaneous measurements conducted 4 km downslope above a subalpine forest, over a period of two summers and one winter. The experiment showed that long-term (measurements are on-going), nearly continuous turbulent flux measurements, with real-time data transmission, can be made at the alpine site. Surface energy balance closure of between 71–91% was achieved, in-part due to the relatively flat ridge-top location, the short flux footprint, and windy conditions. The advection of CO_2 was small, likely due the location on the ridge top away from strong upwind sources of CO_2, persistent windy and turbulent conditions, and the influence of CO_2 drainage flows down the adjacent valleys.

Despite a vertical and horizontal separation of only 430 m and 4 km, respectively, the alpine site had lower air temperatures and higher relative humidity than the forest site, but less than that explained by the dry adiabatic lapse rate. Both sites were windy, with higher mean wind speeds at the alpine site, and downslope winds prevailed at the alpine site compared to a diurnal switch to daytime upslope flows at the forest site.

The comparison between the surface energy balance components at each site showed the net radiation was higher over the forest (lower albedo), as was the sensible heat flux, especially in early in the winter. The latent heat flux at the alpine site was consistently less than that over the forest, yet the evaporative fraction was similar between the two sites, indicating similar partitioning of the available energy between latent and sensible heat. Although the magnitude of the soil heat flux was relatively small at both sites, it was greater at the alpine site, indicative of the low *LAI* and high fraction of exposed ground.

Calculating *NEE* at the alpine with or without accounting for horizontal advection either directly or by using a friction velocity-based filter did not have a significant effect on cumulative *NEE* estimates. The meteorological differences observed at the sites, namely windy, cooler conditions at the alpine site, resulted in a 108 day shorter negative (net uptake) *NEE* period, and a 96 day longer positive (net loss) *NEE* period, compared to the forest site. The ecosystem water use efficiency was more than three-times greater at the forest site compared to the alpine site, given the longer growing season, greater leaf area index, and presumably lower levels of climate-induced physiological stress.

The eddy covariance method of measuring the turbulent exchange of water and carbon dioxide has the advantage of continuously sampling relatively large areas with minimal disturbance. With suitable site selection and experimental design, this paper shows that this method can be used to make reliable measurements of surface-atmosphere interactions at a high elevation alpine tundra site situated in complex terrain. Over the bulk of the growing season, results show that the alpine tundra played a contrasting yet significant role in water and CO_2 exchange despite its low leaf area index. It is hoped that these results will be used to calibrate and validate both modeling tools and remote sensing products for use in predicting the responses of alpine tundra to climate change.

Acknowledgments The research was supported by NSF-LTER (Grant DEB 0423662), and grants to RKM from the Western Section of the National Institute for Climate Change Research (NICCR) (Award MPC35TX-A2) administered by Northern Arizona University, and the U.S. National Science Foundation (Grant EAR 0321918). The helpful comments and suggestion from the three anonymous reviewers greatly improved the quality and presentation of this manuscript.

References

Aubinet M, Grelle A, Ibrom A, Rannick U, Moncrief J, Foken T, Kowalski AS, Martin PH, Berbigier P, Bernhofer C,

Clement R, Elbers J, Granier A, Grunwald T, Morgenstern K, Pilegaard K, Rebmann C, Snijders W, Valentini R, Vesala T (2000) Estimates of the annual net carbon and water exchange of forests: the EUROFLX methodology. Adv Ecol Res 30:113–175. doi:10.1016/S0065-2504(08)60018-5

Aubinet M, Heinesch B, Yernaux M (2003) Horizontal and vertical CO_2 advection in a sloping forest. Bound Lay Meteorol 108:397–417. doi:10.1023/A:1024168428135

Baker WL, Veblen TT, Sherriff RL (2007) Fire, fuels and restoration of ponderosa pine-Douglas fir forests in the Rocky Mountains, USA. J Biogeogr 34:251–269. doi:10.1111/j.1365-2699.2006.01592.x

Barry RG (2008) Mountain weather and climate, 3rd edn. Cambridge University Press, Cambridge 506 pp

Beniston M, Diaz HF, Bradley RS (1997) Climatic change at high elevation sites: an overview. Clim Change 36:233–251. doi:10.1023/A:1005380714349

Bowling DR, Massman WJ, Schaeffer SM, Burns SP, Monson RK, William MW (2009) Biological and physical influences on the carbon isotope content of CO_2 in a subalpine forest snowpack, Niwot Ridge, Colorado. Biogeochemistry (this issue). doi:10.1007/s10533-008-9233-4

Burba GG, McDermitt DK, Grelle A, Anderson DJ, Xu L (2008) Addressing the influence of instrument surface heat exchange on the measurements of CO_2 flux from open-path gas analyzers. Glob Chang Biol 14(8):1854–1876. doi:10.1111/j.1365-2486.2008.01606.x

Cline DW (1997) Snow surface energy exchanges and snowmelt at a continental midlatitude Alpine site. Water Resour Res 33(4):689–701. doi:10.1029/97WR00026

Daly C, Shankman D (1985) Seedling establishment by conifers above tree limit on Niwot Ridge, Front Rage, Colorado, USA. Arct Alp Res 17:389–400. doi:10.2307/1550864

Elliot GP, Baker WL (2004) Quaking aspen (populus tremuloides Michx.) at tree line: a century of change in the San Juan Mountains, Colorado, USA. J Biogeogr 31:733–745

Feigenwinter C, Bernhofer C, Vogt R (2004) The influence of advection on the short term CO_2 budget in and above a forest canopy. Bound Lay Meteorol 113:201–224. doi:10.1023/B:BOUN.0000039372.86053.ff

Feigenwinter C et al (2008) Comparison of horizontal and vertical advective CO_2 fluxes at three forest sites. Agric For Meteorol 148:12–24. doi:10.1016/j.agrformet.2007.08.013

Gehrig-Fasel J, Guisan A, Zimmermann NE (2007) Tree line shifts in the swiss alps: climate change or land abandonment? J Veg Sci 18:571–582

Goulden ML, Munger JW, Fan S-M, Daube BC, Wofsy SC (1996) Measurements of carbon sequestration by long-term eddy covariance: methods and critical evaluation of accuracy. Glob Chang Biol 2:169–182. doi:10.1111/j.1365-2486.1996.tb00070.x

Gu S, Tang YH, Cui XY, Du M, Zhao L, Li Y, Xu SX, Zhou H, Kato T, Qi PT, Zhao X (2008) Characterizing evapotranspiration over a meadow ecosystem on the Qinghai-Tibetan Plateau. J Geophys Res–Atmos, 113: D08118, doi:10.1029/2007JD009173

Hammerle A, Haslwanter A, Schmitt M, Bahn M, Tappeiner U, Cernusca A, Wohlfahrt G (2007) Eddy covariance measurements of carbon dioxide, latent and sensible energy fluxes above a meadow on a mountain slope. Bound Lay Meteorol 122:397–416. doi:10.1007/s10546-006-9109-x

Humphries HC, Coffin DP, Laurenroth WK (1996) An individual-based model of alpine plant distributions. Ecol Modell 84:99–126. doi:10.1016/0304-3800(94)00144-8

Jarlan L, Balsmo G, Lafont S, Beljaars A, Calvet JC, Mougin E (2008) Analysis of leaf area index in the ECMWF land surface model and impact on latent heat and carbon fluxes: application to West Africa. J Geophys Res-Atmos 113: Article D24117

Keller F, Kienast F, Beniston M (2000) Evidence of response of vegetation to environmental change on high-elevation sites in the Swiss Alps. Reg Environ Change 1:70–77. doi:10.1007/PL00011535

Kerwin MW, Overpeck JT, Webb RS, Anderson KH (2004) Pollen-based summer temperature reconstructions for the eastern Canadian boreal forest, subarctic, and Arctic. Quat Sci Rev 23:1901–1924. doi:10.1016/j.quascirev.2004.03.013

Kittel T, Chowanski K, Ackerman T (2007) Long-term climate record. Niwot Ridge LTER NSF Report, June 2007

Körner C (2003) Alpine plant life–functional plant ecology of high mountain ecosystems, 2nd edn. Springer, Berlin

Kutsch W, Kolle O, Rebmann C, Knohl A, Ziegler W, Schulze E-D (2008) Advection and resulting CO_2 exchange uncertainty in a tall forest in central Germany. Ecol Appl 18(6):1391–1405. doi:10.1890/06-1301.1

Lee X, Massman W, Law B (2004) Handbook of micrometeorology: a guide for surface flux measurements and analysis. Kluwer Academic Publishers, Dordrecht 250 pp

Leuning R, Zegelin SJ, Jones K, Keith H, Hughes D (2008) Measurement of horizontal and vertical advection of CO_2 within a forest canopy. Agric For Meteorol 148:1777–1797. doi:10.1016/j.agrformet.2008.06.006

Lewicki JL, Fisher ML, Hilley GE (2008) Six-week time series of eddy covariance CO_2 flux at Mammoth Mountain, California: performance evaluation and role of meteorological forcing. J Volcanol Geotherm Res 171:178–190. doi:10.1016/j.jvolgeores.2007.11.029

MacDonald GM, Edwards TWD, Moser DA, Pienitz R, Smol JP (1993) Rapid response of tree line vegetation and lakes to past climate warming. Nature 361:243–246. doi:10.1038/361243a0

McMillen RT (1988) An eddy correlation technique with extended applicability to non-simple terrain. Bound Lay Meteorol 43:231–245. doi:10.1007/BF00128405

Molotch NP, Blanken PD, Williams M, Turnipseed A, Monson R, Margulis S (2007) Estimating sublimation of intercepted and sub-canopy snow using eddy covariance systems. Hydrol Process 21(12):1567–1575. doi:10.1002/hyp.6719

Monson RK, Turnipseed AA, Sparks JP, Harley PC, Scott-Denton LE, Sparks K, Huxman TE (2002) Carbon sequestration in a high-elevation subalpine forests. Glob Chang Biol 8:459–478. doi:10.1046/j.1365-2486.2002.00480.x

Monson RK, Lipson DL, Burns SP, Turnipseed AA, Delany AC, Williams MW, Schmidt SK (2006) Winter forest soil respiration controlled by climate and microbial community composition. Nature 439:711–714. doi:10.1038/nature04555

Motta R, Nola P (2001) Growth trends and dynamics in subalpine forest stand in the Varaita Valley (Piedmont, Italy)

and their relationships with human activities and global change. J Veg Sci 12:219–230. doi:10.2307/3236606

Negron JF, Popp JB (2004) Probability of ponderosa pine infestation by mountain pine beetle in the Colorado Front Range. For Ecol Manage 191:17–27. doi:10.1016/j.foreco.2003.10.026

Pauli H, Gottfried M, Grabherr G (2001) High summits of the Alps in a changing climate. The oldest observation series on high mountain plant diversity in Europe. In: Walther GR, Burga CA, Edwards PJ (eds) Fingerprints of climate change. Adapted behaviour and shifting species ranges. Kluwer Academic/Plenum Publishers, New York, pp 139–149

Paulsen J, Weber UM, Körner C (2000) Tree growth near tree line: abrupt or gradual reduction with altitude? Arct Antarct Alp Res 32:14–20. doi:10.2307/1552405

Schuepp PH, Leclerc MY, MacPherson JI, Desjardins RL (1990) Footprint prediction of scalar fluxes from analytical solutions of the diffusion equation. Bound Lay Meteorol 50:353–373

Seastedt T, Bowman B, Caine N, McKnight D, Townsend A, Williams MW (2004) The landscape continuum: a conceptual model for high elevation ecosystems. BioScience 54(2):111–121

Sherriff RL, Veblen TT, Sibold JS (2001) Fire history in high elevation subalpine forests in the Colorado Front Range. Ecosicence 8:369–380

Shi X, Xu LL, HE YT, Zhang XZ, Zhang DQ, Yu GR (2006) Net ecosystem CO_2 exchange and controlling factors in a steppe-Kobresia meadow on the Tibetan Plateau. Sci China Ser D- Earth Sci 49:207–218

Sievering H, Tomaszewski T, Torizzo J (2007) Canopy uptake of atmospheric N deposition at a conifer forest: Part 1-Canopy N budget, photosynthetic efficiency and net ecosystem exchange. Tellus Ser B 59:483–492. doi:10.1111/j.1600-0889.2007.00264.x

Staebler RM, Fitzjarrald DR (2004) Observing subcanopy CO_2 advection. Agric For Meteorol 122:139–156. doi:10.1016/j.agrformet.2003.09.011

Sun J, Mahrt L (1994) Spatial-distribution of surface fluxes estimated from remotely sensed variables. J Appl Meteorol 33(11):1341–1353. doi:10.1175/1520-0450(1994)033<1341:SDOSFE>2.0.CO;2

Sun J, Burns SP, Delany AC, Oncley SP, Turnipseed AA, Stephns BB, Lenschow DH, LeMone MA, Monson RK, Anderson DE (2007) CO_2 transport over complex terrain. Agric For Meteorol 145:1–21. doi:10.1016/j.agrformet.2007.02.007

Turnipseed AA, Blanken PD, Anderson DE, Monson RK (2002) Energy budget above a high-elevation subalpine forest in complex terrain. Agric For Meteorol 110:177–201. doi:10.1016/S0168-1923(01)00290-8

Turnipseed AA, Anderson DE, Burns S, Blanken PD, Baugh WM, Monson RK (2003) Airflows and turbulent flux measurements in mountainous terrain, Part I. Canopy and local effects. Agric For Meteorol 119:1–21. doi:10.1016/S0168-1923(03)00136-9

Turnipseed AA, Anderson DE, Burns S, Blanken PD, Monson RK (2004) Airflows and turbulent flux measurements in mountainous terrain, Part II. Mesoscale effects. Agric For Meteorol 125:187–205. doi:10.1016/j.agrformet.2004.04.007

Walker MD, Walker DA, Theodose TA, Webber PJ (2001) The vegetation: hierarchical species-environment relationships. In: Bowman WD, Seastedt TR (eds) Structure and function of an alpine ecosystem: Niwot Ridge, Colorado. Oxford University Press, New York

Walther G-R, Beissner S, Burga CA (2005) Trends in the upward shift of alpine plants. J Veg Sci 16:541–548

Wang W, Davis KJ, Cook BD, Bakwin PS, Chuixiang Y, Butler MP, Ricciuto DM (2005) Surface layer CO_2 budget and advective contributions to measurements of net ecosystem-atmosphere exchange of CO_2. Agr For Meteorol 135:202–214

Wilczak JM, Oncley SP, Stage SA (2001) Sonic anemometer tilt correction algorithms. Bound Lay Meteorol 99:127–150

Williams MW, Losleben M, Hamann H (2002) Alpine areas in the colorado front range as monitors of climate change and ecosystem response. Geogr Rev 92:180–191

Yi C, Anderson DE, Turnipseed AA, Burns SP, Sparks JP, Stannard DI, Monson RK (2008) The contribution of advective fluxes to net ecosystem CO_2 exchange in a high-elevation, subalpine forest. Ecol Appl 18:1379–1390